NANO LETTERS

Letter

pubs.acs.org/NanoLett

Plasmon Field Effect Transistor for Plasmon to Electric Conversion and Amplification

Hossein Shokri Kojori,[†] Ju-Hyung Yun,[‡,§] Younghun Paik,[†] Joondong Kim,[§] Wayne A. Anderson,[‡] and Sung Jin Kim*[,†,∥]

[†]Department of Electrical and Computer Engineering, University of Miami, Miami, Florida 33124, United States

[‡]Department of Electrical Engineering, The State University of New York at Buffalo, Buffalo, New York 14260, United States

[§]Department of Electrical Engineering, Incheon National University, Incheon 13559, Korea

[∥]Biomedical Nanotechnology Institute (BioNIUM), University of Miami, Miami, Florida 33124, United States

Supporting Information

ABSTRACT: Direct coupling of electronic excitations of optical energy via plasmon resonances opens the door to improving gain and selectivity in various optoelectronic applications. We report a new device structure and working mechanisms for plasmon resonance energy detection and electric conversion based on a thin film transistor device with a metal nanostructure incorporated in it. This plasmon field effect transistor collects the plasmonically induced hot electrons from the physically isolated metal nanostructures. These hot electrons contribute to the amplification of the drain current. The internal electric field and quantum tunneling effect at the metal−semiconductor junction enable highly efficient hot electron collection and amplification. Combined with the versatility of plasmonic nanostructures in wavelength tunability, this device architecture offers an ultrawide spectral range that can be used in various applications.

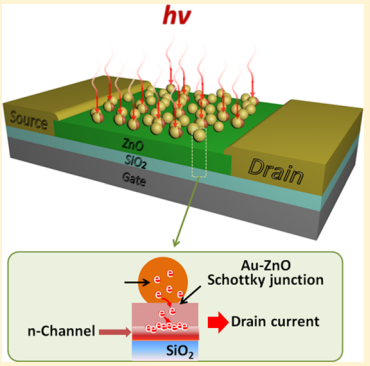

KEYWORDS: *localized surface plasmon resonance, plasmon energy detection, plasmon field effect transistor, nanophotonics*

Recent advances in nanotechnology have made subwavelength nanostructures a reality and various nanomaterials, fabrication techniques, and characterization methods have been utilized to successfully demonstrate plasmonic effects in a myriad of applications such as metamaterials,[1−4] photovoltaic devices,[5−9] spectroscopy,[10−14] localized heat generation for medical therapy,[15−17] quantum optics,[9,18,19] and plasmonic circuits.[4,20,21] One of the key functions for the use of the plasmonic effect is an efficient conversion of plasmon energy to an electrical signal or vice versa. A metal−semiconductor junction structure enables plasmonic energy detection as a form of electrical current.[6,22−26] Photons absorbed in a metal nanostructure generate hot electrons and the electrons can cross by thermionic diffusion at the boundary between metal and semiconductor resulting in photocurrent or energy band modification in semiconductors.[27−34] There have been various types of plasmonic energy detection using diode or transistor structures. However, these detectors are limited by low quantum efficiency due to low absorption in the thin metal structure and inefficient hot electron diffusion from metal to semiconductor.[26−28,35,36] Recently, Li et al. have reported significant improvement regarding the responsivity of hot electron detection. A perfect absorber with novel nano geometry enables photoresponsivity to jump up to several mA/W from the conventional detection range of a few tens to 100 μA/W.[37] Here, we achieved drastic increase of photo responsivity in the order of A/W with plasmon energy amplification.[38]

We report a device, plasmon−field-effect transistor (FET), and working mechanisms for plasmon resonance energy detection and simultaneous amplification process. The plasmon−FET collects plasmonically induced hot electrons from the metal nanostructures, and these hot electrons contribute to the amplification of the drain current by modulating the channel conductivity. Moreover, the gate voltage bias controlled internal electric field and quantum tunneling effect at the metal−semiconductor junction enable efficient hot electron collection and amplification. We achieved more than 3 A/W of responsivity at the peak wavelength of plasmonic absorption, and it is the first demonstration of a plasmonic detector with a controlled amplification function. The unique design of the plasmon−FET provides several advantages such as physical separation between plasmonic nanostructures and the electrodes, highly efficient amplification of detected plasmon energy, and detection capability of lower energy photons using a quantum tunneling mechanism. Therefore, the plasmon−FET holds great promise in many applications such as a bridge device between photonics and

Received: September 8, 2015
Revised: December 2, 2015

ACS Publications © XXXX American Chemical Society

DOI: 10.1021/acs.nanolett.5b03625
Nano Lett. XXXX, XXX, XXX−XXX

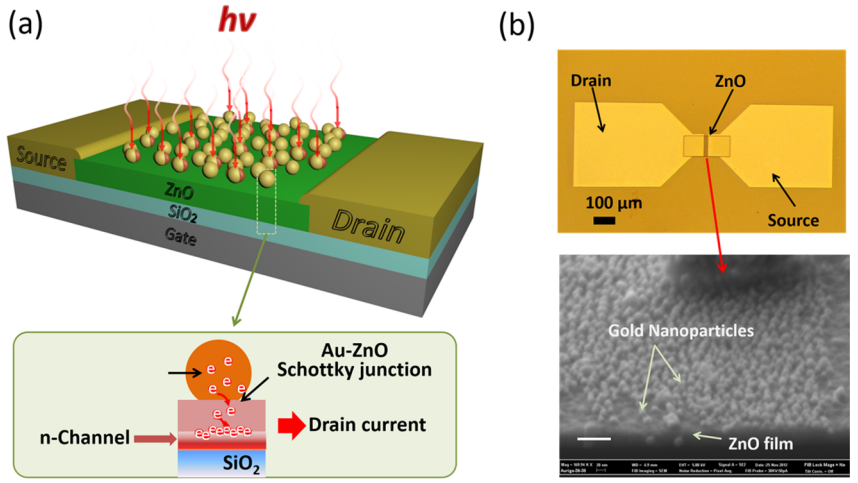

Figure 1. Plasmon FET for highly efficient plasmon energy detection. (a) Illustration of plasmon FET structure and operational principle of plasmon FET under light illumination. The plasmon-induced hot electrons migrate from gold nanostructure to ZnO channel and increase channel conductivity and drain current. (b) Picture of the fabricated device: optical microscope image (top) and scanning electron microscopy (SEM) image of ZnO channel with gold NPs (bottom).The scale bar in the SEM picture is 80 nm.

electronics, highly sensitive chemical/biological sensors, and detectors for UV to IR spectral response.

The plasmon−FET is fabricated using a ZnO thin film FET structure, as shown in Figure 1a. A heavily doped n-type Si substrate serves as a back gate and an n-type ZnO film deposited on thermally grown SiO_2 serves as an active semiconductor channel. Prior to incorporating the gold nanostructures, electrical characterization is carried out for all fabricated ZnO FET devices. The plasmonic energy detection capability is added by incorporating gold nanoparticles (NPs) on the active ZnO channel of the FET. As confirmed by SEM image in Figure 1b and atomic force microscopy (AFM) study (see page 9 of the Supporting Information), the gold NPs are physically isolated from all three electrodes, which allows great flexibility on the design of functional nanostructure. Furthermore, gold NPs can be exposed to an aqueous solution with proper passivation on drain and source electrodes. This is one of the advantages of plasmon FETs for sensor application for liquid samples. On the basis of the work function difference between gold and n-type ZnO, it is expected that a Schottky barrier is formed with around 0.6−0.7 eV of barrier height (see page 10 of the Supporting Information). Thus, the generated hot electrons with higher energy than this Schottky barrier can thermionically diffuse from gold NPs to the ZnO layer. In terms of optical properties, the gold NPs with 5−10 nm in radius exhibit strong plasmonic absorption around a wavelength of ∼520 nm.[39] This absorption peak depends on the dielectric constant of the host material surrounding gold NPs and on the shape and size of NPs. In order to avoid overlap of the absorption spectrum, we choose ZnO for the FET channel material. We confirm that the bandgap of 250 nm thick ZnO thin film is 3.3 eV and shows almost zero absorbance (<0.001%) at the spectral range between 450 to 1100 nm. Thus, it is expected that there will be no optical response in the drain current under illumination at any visible wavelength.

As discussed earlier, the plasmonic absorption generates hot electrons in gold NPs and these energetic hot electrons can migrate across the Schottky barrier and diffuse to the ZnO film (Figure 1a). Consequently, this process supplies more electrons in the ZnO channel, resulting in increased channel conductivity and drain current (I_d). Because the number of migrated hot electrons depends on the plasmonic absorption of gold NPs, the expected drain current response as a function of wavelength should be matched with the absorption spectrum of gold NPs. Therefore, the plasmon−FET converts localized surface plasmon energy to electrical charges and their flow. Furthermore, plasmon energy was amplified with gate voltage bias, facilitating quantum tunneling of electrons from gold NPs into the ZnO channel.

To confirm the working principle, we carried out a set of optical and electrical measurement using three different samples: a gold NPs deposited glass substrate, a FET without gold NPs, and a gold NPs incorporated plasmon−FET. These samples were fabricated using identical fabrication processes. First, the plasmonic absorbance of gold NPs on a glass substrate was measured. Next, we carried out an experiment by manipulating the refractive index surrounding the gold nanoparticles using 3-mercaptopropionic acid (MPA). 3-MPA has a higher refractive index than air (n = 1.492) and binds well with the gold surface due to the thiol(—SH)-terminated structure. The 3-MPA coating increases the average refractive index for surrounding matrix on gold NPs and consequently induces a red shift in the plasmonic absorption spectrum, which is displayed in Figure 2a (see page 2 of the Supporting Information). The same functionalization procedure was used to change the refractive index of surrounding media of the gold NPs in the plasmon−FET. The control FET device without gold NPs did not produce any photocurrent, whereas the plasmon−FET has a well matched spectral response with the plasmonic absorption of gold NPs, as shown in Figure 2b. In addition, simulation based on a finite differential time domain (FDTD) supports this measured spectral response (see Figure S3 of the Supporting Information). We also observed a slight change of spectral response when the incident angle of the light was changed because of the semispherical shape of the gold nanoparticles (see Figure S4 of the Supporting Information). The slight discrepancy of the wavelength of the absorption peaks between the glass substrate and plasmon−FET is due to the difference in refractive index of ZnO film where the gold nanoparticles are self-assembled. These results show that the plasmon−FET enables direct conversion of the absorbed plasmon resonance energy from the gold NPs. Additionally,

DOI: 10.1021/acs.nanolett.5b03625
Nano Lett. XXXX, XXX, XXX−XXX

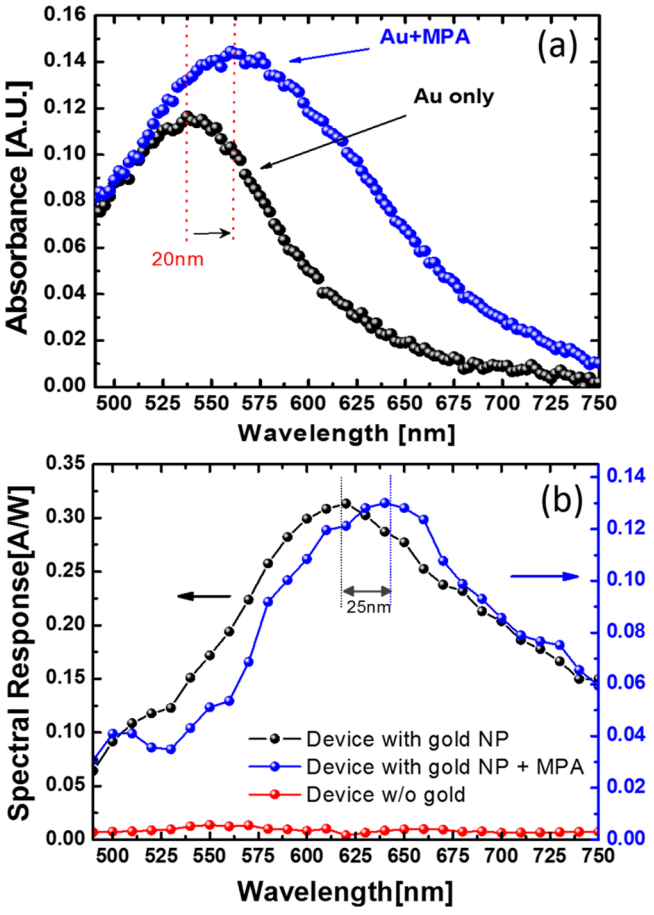

Figure 2. Optoelectrical properties of the plasmon FET. (a) Absorption spectra of bare gold nanoparticles and 3-MPA coated gold nanoparticles. The nanoparticles are deposited on a glass substrate. (b) Spectral response of the plasmon FET: the spectral responses are taken from a FET without gold NPs, after gold NP incorporation and after 3-MPA molecule attached on gold NPs. The spectral responses of plasmon FET were recorded at each condition using the same device.

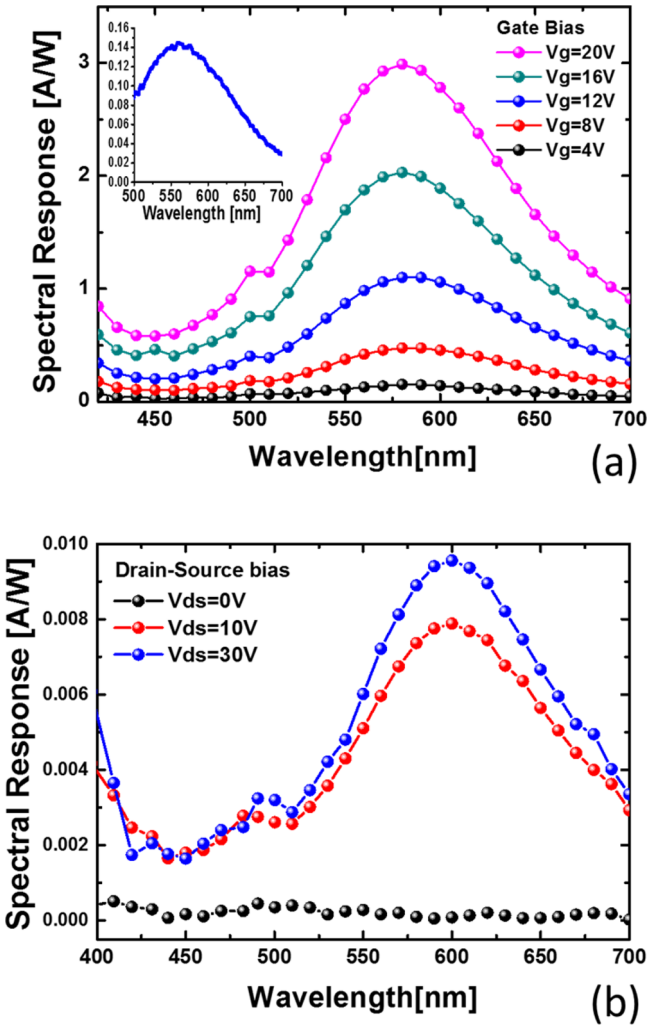

Figure 3. Spectral response (A/W) of the plasmon FET. (a) Under different gate voltage bias conditions. The inset shows the absorption spectrum of gold NPs a ZnO film/glass substrate (the drain−source bias voltage is 20 V). The converted external quantum efficiency with amplification is shown in Figure S12. (b) Spectral response as a function of drain−source voltage under a zero gate voltage bias.

we note that the refractive index change associated with the small molecule functionalization on the gold nanoparticles altered its spectral response, opening up opportunities for an integrated plasmon based biological or chemical sensing platform.

One of the most exiting properties of the plasmon−FET is the amplification of plasmon detection, which is not reported elsewhere. We demonstrated amplified plasmonic spectral response from the plasmon−FET using gold NPs. The spectral response (A/W) as a function of wavelength depends on the gate voltage bias as shown in Figure 3a. Under the saturation mode operation of the plasmon FET, the spectral responsivity reached higher than 3 A/W. (The converted external quantum efficiency with gain mechanism is shown in Figure S12.) However, the plasmon FET has a very poor spectral response (less than 0.01) when there was no gate voltage applied as shown in Figure 3b. Without gate bias voltage, the induced plasmonic hot electrons can be transferred to semiconductor, but this mechanism has a very low quantum efficiency because only diffusion process is involved. We also confirmed that there is no observable plasmonic response when the opposite electrical potential (negative gate bias) was applied (see Figure S5 of the Supporting Information). This efficient amplification and gate bias controlled response can be explained by an energy band model. Without gate voltage bias as shown in Figure 4a, the plasmon induced hot electrons can migrate only with diffusion once they have high enough energy to overcome the Schottky barrier (process ① in Figure 4a,b).[31−33] These diffused hot electrons could be collected by the electric field across the drain and source as a drift current. ($I_{drift} = \sigma E$, where σ is the conductivity of ZnO channel and E is electric field.) The stronger electric field produced by the drain−source voltage bias can increase the drift current (Figure 3b). When positive gate voltage is applied to the plasmon−FET, electron accumulation layer (n-channel) is formed inside ZnO in the vicinity of the SiO_2 layer. The spatial difference of electron density generates a large potential gradient from the floating ground (metal nanostructure) to electron accumulation region as illustrated in Figure 4b. This internal electric field created by the gate bias facilitates electrons to move to the other boundary where the FET channel is located (process ③ in Figure 4b). The migrated hot electrons are seized by the gate voltage, consequently contributing to channel enhancement and allowing more drain current to flow (process ④ in Figure

DOI: 10.1021/acs.nanolett.5b03625
Nano Lett. XXXX, XXX, XXX−XXX

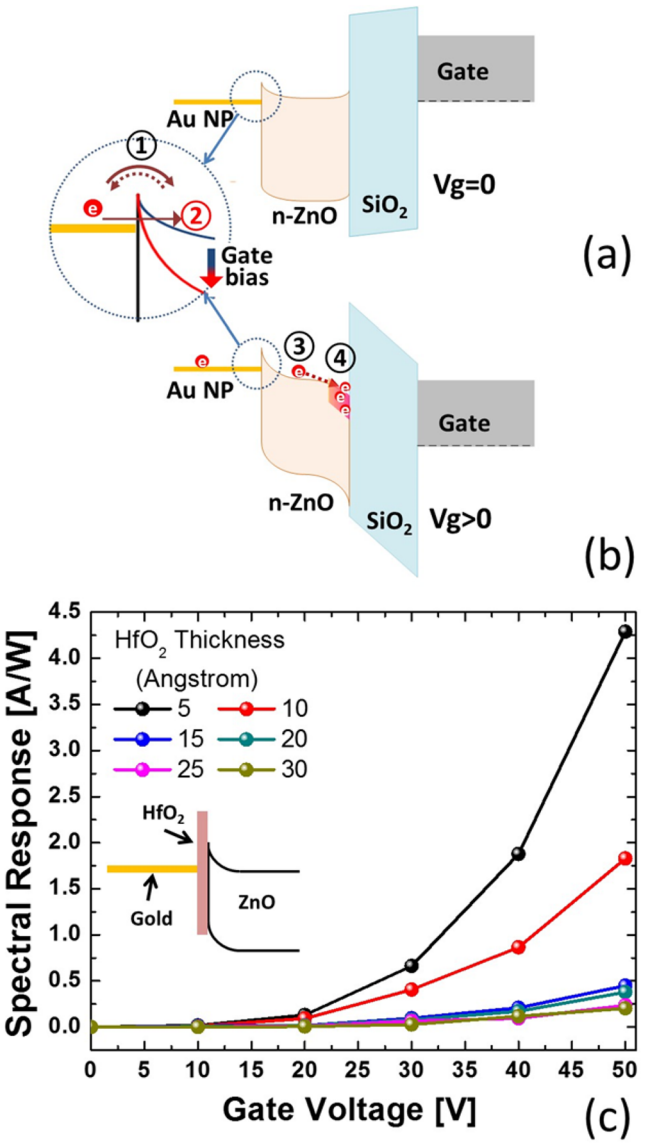

Figure 4. Gate voltage dependent ZnO energy band bending of a plasmon FET and amplification mechanism. (a) Thermionic diffusion without gate bias. (b) Internal field assisted hot electron migration and quantum tunneling at the Schottky junction with gate voltage bias. (c) Measured Drain current from plasmon FETs with various thickness of HfO_2 film between gold and ZnO layer. Each data point is taken from the peaks of the spectral responses.

4b). Therefore, the collected drain current is proportional to the plasmonic absorption from the gold nanostructure, but is not saturated due to the limited number of hot electrons generated in the metal. It should be noted that the free electrons in the gold nanostructure were not depleted after long time exposure to the light. (see Figure S6 of the Supporting Information) This could indicate that there is a restoring force to recharge electrons back in gold NPs because nanoparticles are attached to the ZnO surface, which has an electric field by drain−source voltage bias at their boundary. In the Supporting Information, we discussed more details about the restoring force based on findings from our empirical studies. However, further investigation is needed to understand how fast and efficiently the gold NPs restore the electrons under the complex device structure and internal field conditions. Furthermore, the importance of gate bias assisted hot electron accumulation has been studied using devices with different ZnO channel thicknesses, and it shows that a stronger electric field is important for efficient plasmon energy detection (see Figure S10 of the Supporting Information). We calculated the efficiency of hot electron contribution to the increased drain current. Interestingly, this internal quantum efficiency varies from 5% to 17% when the applied gate voltage bias is increased from 4 to 20 V, respectively (see Figure S8 of the Supporting Information). This is a unique property of the plasmon FET since the light absorption occurs outside of the semiconductor channel. Under the 20 V bias for both gate and drain−source in Figure 3a, the number of hot electrons contributed to the drain current is 8.6×10^8, whereas the number of absorbed photons is 5.05×10^9 at 580 nm. Therefore, assuming we have 20 nm gold NPs, each gold NP generates 72 contributing hot electrons to the amplified drain current (see page 7 of the Supporting Information). When gate bias is applied, there is another interesting hot electron migration mechanism, which is a quantum tunneling process through the thin Schottky barrier (process ② in Figure 4a,b). The modified potential from the positive gate bias creates not only a drift field to facilitate hot electron migration but also a thin enough Schottky barrier to allow electron tunneling from gold NPs to ZnO channel.

In order to confirm this tunneling mechanism, we manipulated the thickness of tunnel barrier by introducing different thickness of insulator (HfO_2-layer with 5−30 Å) at the Schottky junction (between gold and ZnO). Generally, a barrier thinner than 10−30 Å induce tunneling of electrons.[40−42] Otherwise, only thermionic injection of electrons is allowed over the barrier. Plasmon FETs with the insulating layer with 5−10 Å of HfO_2 thickness also show similar drain current amplification as a function of gate voltage bias, as shown in Figure 4c. However, drain current was drastically suppressed with a thick barrier (15−30 Å thick HfO_2) compared with a thin barrier (5−10 Å). Depending on an overall barrier thickness, $T_{Overall} = T_{HfO_2}$ (fixed) + $T_{Schottky}$ (decreased with increasing gate bias), drain current was significantly changed at identical gate bias. The probability of quantum tunneling is an exponential function ($T \sim e^{-2\gamma L}$, where T is the probability of tunneled electrons, γ is wavenumber or absorption coefficient inside barrier and L is the barrier length[43,44]). The measured drain current was decreased exponentially as the HfO_2 thickness is increased. These results were well matched with the expectation of tunneling induced hot electron migration and confirmed that quantum tunneling is one of the mechanisms of hot electron migration from the metal nanostructures to the ZnO channel. Therefore, we can conclude that tunneling-assisted hot electron migration may enable a plasmon FET to detect photon energy that is below the Schottky barrier energy of 0.6−0.7 eV.

In summary, we have successfully demonstrated a new device that enables highly efficient plasmon energy detection accompany with gate-bias controlled amplification process. Gate bias modifies energy band and facilitates efficient migration of plasmon induced hot electrons over and through the Schottky barrier. The internal field in the ZnO layer also allows efficient collection of these hot electrons to increase its channel conductivity and, consequently, drain current. The physically isolated nanostructures can be functionalized using chemicals or biological molecules for the bio/chemical sensor applications. In addition, the unique quantum tunneling at the Schottky junction enables to detect the electromagnetic wave

DOI: 10.1021/acs.nanolett.5b03625
Nano Lett. XXXX, XXX, XXX−XXX

that is lower than Schottky barrier energy which would be useful in many applications such as imaging, plasmonic integrated circuits, and detection technology for UV to THz spectrum.

■ ASSOCIATED CONTENT

Supporting Information

The Supporting Information is available free of charge on the ACS Publications website at DOI: 10.1021/acs.nanolett.5b03625.

Experimental details (device fabrication and characterization), FDTD simulation results of plasmon response, power and incident angle dependence in spectral response of plasmon FET, spectral response under negative gate bias, extra study on free electron discharging, calculation of internal quantum efficiency, atomic force microscopy image of gold nanostructure, spectral response from the devices with various channel thickness, and study on Au/ZnO Schottky barrier height. (PDF)

■ AUTHOR INFORMATION

Corresponding Author

*E-mail: kim@miami.edu.

Author Contributions

H.S.K and J.-H.Y. contributed equally.

H.S.K., J.-H.Y. and S.J.K. designed and performed the experiments and analyzed the data. H.S.K., J.-H.Y., J.K. and S.J.K fabricated the devices. H.S.K. performed the numerical simulations. Y.P. assisted in the experiments. H.S.K., J.-H.Y., W.A.A. and S.J.K wrote the manuscript. S.J.K. developed and supervised the project.

Notes

The authors declare no competing financial interest.

■ ACKNOWLEDGMENTS

The Authors thank Drs. Brett Wenner and Monica Allen at Air Force Research Laboratory for their helpful discussions. This work was partially supported by John T. Macdonald Foundation Biomedical Nanotechnology Institute and NSF Grant #1235036. A related U.S. patent application has been filed.

■ REFERENCES

(1) Boltasseva, A.; Atwater, H. A. *Science* **2011**, *331* (6015), 290−291.
(2) Drachev, V. P.; Chettiar, U. K.; Kildishev, A. V.; Yuan, H.-K.; Cai, W.; Shalaev, V. M. *Opt. Express* **2008**, *16* (2), 1186−1195.
(3) Henzie, J.; Lee, M. H.; Odom, T. W. *Nat. Nanotechnol.* **2007**, *2* (9), 549−554.
(4) Kabashin, A. V.; Evans, P.; Pastkovsky, S.; Hendren, W.; Wurtz, G. A.; Atkinson, R.; Pollard, R.; Podolskiy, V. A.; Zayats, A. V. *Nat. Mater.* **2009**, *8* (11), 867−871.
(5) Atwater, H. A.; Polman, A. *Nat. Mater.* **2010**, *9* (3), 205−213.
(6) Knight, M. W.; Sobhani, H.; Nordlander, P.; Halas, N. J. *Science* **2011**, *332* (6030), 702−704.
(7) Okamoto, K.; Niki, I.; Shvartser, A.; Narukawa, Y.; Mukai, T.; Scherer, A. *Nat. Mater.* **2004**, *3* (9), 601−605.
(8) Ferry, V. E.; Munday, J. N.; Atwater, H. A. *Adv. Mater.* **2010**, *22* (43), 4794−4808.
(9) Schuller, J. A.; Barnard, E. S.; Cai, W.; Jun, Y. C.; White, J. S.; Brongersma, M. L. *Nat. Mater.* **2010**, *9* (3), 193−204.
(10) Haes, A. J.; Haynes, C. L.; McFarland, A. D.; Schatz, G. C.; Van Duyne, R. P.; Zou, S. *MRS Bull.* **2005**, *30* (05), 368−375.
(11) Mulvaney, P. *Langmuir* **1996**, *12* (3), 788−800.
(12) Sherry, L. J.; Chang, S.-H.; Schatz, G. C.; Van Duyne, R. P.; Wiley, B. J.; Xia, Y. *Nano Lett.* **2005**, *5* (10), 2034−2038.
(13) Sherry, L. J.; Jin, R.; Mirkin, C. A.; Schatz, G. C.; Van Duyne, R. P. *Nano Lett.* **2006**, *6* (9), 2060−2065.
(14) Willets, K. A.; Van Duyne, R. P. *Annu. Rev. Phys. Chem.* **2007**, *58* (1), 267−297.
(15) Baffou, G.; Quidant, R.; Girard, C. *Appl. Phys. Lett.* **2009**, *94* (15), 153109.
(16) Liao, H.; Nehl, C. L.; Hafner, J. H. *Nanomedicine* **2006**, *1* (2), 201−208.
(17) Pissuwan, D.; Valenzuela, S. M.; Cortie, M. B. *Trends Biotechnol.* **2006**, *24* (2), 62−67.
(18) Bergman, D. J.; Stockman, M. I. *Phys. Rev. Lett.* **2003**, *90* (2), 027402.
(19) Chang, D. E.; Sørensen, A. S.; Hemmer, P. R.; Lukin, M. D. *Phys. Rev. Lett.* **2006**, *97* (5), 053002.
(20) Engheta, N.; Salandrino, A.; Alù, A. *Phys. Rev. Lett.* **2005**, *95* (9), 095504.
(21) Ozbay, E. *Science* **2006**, *311* (5758), 189−193.
(22) Lee, Y. K.; Jung, C. H.; Park, J.; Seo, H.; Somorjai, G. A.; Park, J. Y. *Nano Lett.* **2011**, *11* (10), 4251−4255.
(23) Mubeen, S.; Hernandez-Sosa, G.; Moses, D.; Lee, J.; Moskovits, M. *Nano Lett.* **2011**, *11* (12), 5548−5552.
(24) Wang, F.; Melosh, N. A. *Nano Lett.* **2011**, *11* (12), 5426−5430.
(25) Chen, J.; Badioli, M.; Alonso-Gonzalez, P.; Thongrattanasiri, S.; Huth, F.; Osmond, J.; Spasenovic, M.; Centeno, A.; Pesquera, A.; Godignon, P.; Zurutuza Elorza, A.; Camara, N.; de Abajo, F. J. G.; Hillenbrand, R.; Koppens, F. H. L. *Nature* **2012**, *487* (7405), 77−81.
(26) Fang, Z.; Wang, Y.; Liu, Z.; Schlather, A.; Ajayan, P. M.; Koppens, F. H.; Nordlander, P.; Halas, N. J. *ACS Nano* **2012**, *6* (11), 10222−10228.
(27) García de Arquer, F. P.; Mihi, A.; Kufer, D.; Konstantatos, G. *ACS Nano* **2013**, *7* (4), 3581−3588.
(28) Lin, J.; Li, H.; Zhang, H.; Chen, W. *Appl. Phys. Lett.* **2013**, *102* (20), 203109.
(29) Wu, K.; Rodríguez-Córdoba, W. E.; Yang, Y.; Lian, T. *Nano Lett.* **2013**, *13* (11), 5255−5263.
(30) Clavero, C. *Nat. Photonics* **2014**, *8* (2), 95−103.
(31) Li, Z.; Xiao, Y.; Gong, Y.; Wang, Z.; Kang, Y.; Zu, S.; Ajayan, P. M.; Nordlander, P.; Fang, Z. *ACS Nano* **2015**, *9* (10), 10158−10164.
(32) Li, Z.; Ye, R.; Feng, R.; Kang, Y.; Zhu, X.; Tour, J. M.; Fang, Z. *Adv. Mater.* **2015**, *27* (35), 5235−5240.
(33) Zheng, B. Y.; Zhao, H.; Manjavacas, A.; McClain, M.; Nordlander, P.; Halas, N. J. *Nat. Commun.* **2015**, *6*, 7797.
(34) Kang, Y.; Najmaei, S.; Liu, Z.; Bao, Y.; Wang, Y.; Zhu, X.; Halas, N. J.; Nordlander, P.; Ajayan, P. M.; Lou, J.; Fang, Z. *Adv. Mater.* **2014**, *26* (37), 6467−6471.
(35) Knight, M. W.; Wang, Y.; Urban, A. S.; Sobhani, A.; Zheng, B. Y.; Nordlander, P.; Halas, N. J. *Nano Lett.* **2013**, *13* (4), 1687−1692.
(36) Liu, K.; Sakurai, M.; Liao, M.; Aono, M. *J. Phys. Chem. C* **2010**, *114* (46), 19835−19839.
(37) Li, W.; Valentine, J. *Nano Lett.* **2014**, *14* (6), 3510−3514.
(38) Zheng, B. Y.; Wang, Y.; Nordlander, P.; Halas, N. J. *Adv. Mater.* **2014**, *26* (36), 6318−6323.
(39) Link, S.; El-Sayed, M. A. *J. Phys. Chem. B* **1999**, *103* (21), 4212−4217.
(40) Zhang, P. *Sci. Rep.* **2015**, *5*, 9826.
(41) Illera, S.; Prades, J. D.; Cirera, A. *J. Appl. Phys.* **2015**, *117* (17), 174307.
(42) Vogel, E. M.; Ahmed, K. Z.; Hornung, B.; Henson, W. K.; McLarty, P. K.; Lucovsky, G.; Hauser, J. R.; Wortman, J. J. *IEEE Trans. Electron Devices* **1998**, *45* (6), 1350−1355.
(43) Ferry, D. K.; Bird, J. P. *Electronic materials and devices*; Academic Press: Waltham, MA, 2001.
(44) Kasap, S. O. *Principles of electronic materials and devices*; McGraw-Hill: New York, 2006.

DOI: 10.1021/acs.nanolett.5b03625
Nano Lett. XXXX, XXX, XXX−XXX